ACS APPLIED MATERIALS & INTERFACES

Research Article

www.acsami.org

Electromechanical Response from $LaAlO_3/SrTiO_3$ Heterostructures

Chen Li, Yuyuan Cao, Yuhang Bai, Aidong Li, Shantao Zhang, and Di Wu*

National Laboratory of Solid State Microstructures, Department of Materials Science and Engineering, College of Engineering and Applied Sciences, and Collaborative Innovation Center of Advanced Microstructures, Nanjing University, Nanjing 210093, China

Supporting Information

ABSTRACT: $LaAlO_3$ ultrathin films, 10 unit cells in thickness, have been deposited epitaxially on TiO_2-terminated (001) $SrTiO_3$ substrates with various O_2 pressures. Electromechanical response from the $LaAlO_3/SrTiO_3$ heterostructures is studied using combined piezoresponse force microscopy, electrostatic force microscopy, and scanning Kelvin probe microscopy. Oxygen vacancies are found to be responsible for the observed piezoelectric response but only for samples deposited with an oxygen pressure lower than 10^{-5} mbar. However, ambient humidity is demonstrated to have a significant effect on the electromechanical response. The observations are discussed in terms of modulations on the intrinsic electrostriction in LAO/STO by an electric field induced by nonuniform distribution of either oxygen vacancies in the bulk or ionic adsorbates on the surface of LAO.

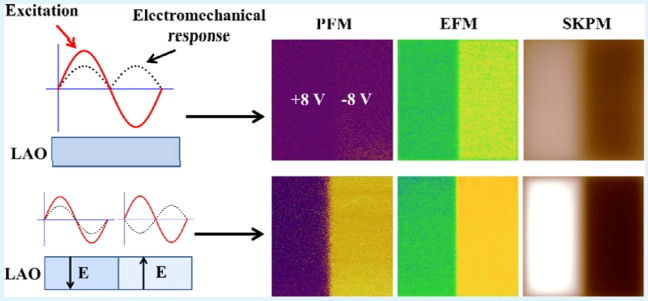

KEYWORDS: *electromechanical response, two-dimentional electron gas, surface adsorbate, piezoresponse force microscopy, surface and interface*

I. INTRODUCTION

Since the discovery of high-mobility two-dimensional electron gas (2DEG) at the interface between perovskite band insulators $LaAlO_3$ (LAO) and $SrTiO_3$ (STO),[1] much attention has been attracted to this unexpected interfacial transport behavior. The origin of this 2DEG has been ascribed to a "polar catastrophe"-driven electron reconstruction induced by the alternating stacking of charged $(LaO)^+$ and $(AlO_2)^-$ atomic layers in LAO upon charge neutral $(SrO)^0$ and $(TiO_2)^0$ atomic layers in STO.[1,2] However, besides the polar catastrophe scenario, electron doping by oxygen vacancies in STO, cation intermixing across the interface, and nonstoichiometry induced during growth are also quoted to account for the observed 2DEG at the LAO/STO interface.[3−14] Although the origin is still in debate, the notable confined conductivity, superconductivity, magnetic properties, and spintronic properties of LAO/STO heterostructures have provided tremendous opportunities for innovation in future oxide electronic devices.[15−25] For example, field effect devices based on LAO/STO interface channels have been fabricated to show potentials for extremely high-density, high-speed transistors.[26] Nonvolatile memory effects have been achieved in LAO/STO heterostructures by using a ferroelectric gate[27] or by injection of surface charges through a conductive atomic force microscope tip.[28−30] Sensors for polar molecules have also been proposed based on the fact that electrostatic boundary conditions in LAO/STO heterostructures vary with surface adsorption, which in turn modulates the interfacial conductivity.[31]

Recently, Bark et al. reported a strong bistable electromechanical response from the surface of LAO/STO heterostructures and attributed it to a dynamic field-induced ionic migration of charged oxygen vacancies.[32] However, Huang et al. attributed the observed hysteresis to variations of the bound states formed by interfacial electron carriers and surface adsorbates.[33] Since neither LAO nor STO are piezoelectric in bulk, this intriguing electromechanical response observed in LAO/STO heterostructures provides a unique opportunity to understand the origin of piezoresponse force signals from thin films and heterostructures. In this Article, we report the electromechanical responses LAO/STO heterostructures as functions of oxygen vacancy concentration, temperature, and ambient humidity, using combined scanning probe techniques such as piezoresponse force microscopy (PFM), electrostatic force microscopy (EFM), and scanning Kelvin probe microscopy (SKPM).

II. EXPERIMENTAL SECTION

A series of LAO ultrathin films, 10 unit cells (u.c.) in thickness, have been deposited on TiO_2-terminated STO substrates by pulsed laser deposition, monitored in situ by reflective high-energy electron diffraction (RHEED). Laser ablation was performed using the 248 nm output of a KrF excimer laser (Compex Pro205 F, Coherent) with a repetition rate of 2 Hz and an energy flux of about 2.0 J/cm^{-2}. During each deposition, the substrate temperature was kept at 750 °C, while the oxygen pressure was maintained at a certain value from 10^{-6} to 10^{-2} mbar. Layer-by-layer epitaxy with clear RHEED intensity oscillations has been achieved to generate an atomically smooth LAO surface showing a step-and-terrace morphology.[39] These 10 u.c.-

Received: December 26, 2014
Accepted: April 28, 2015
Published: April 28, 2015

DOI: 10.1021/am509113j
ACS Appl. Mater. Interfaces 2015, 7, 10146−10151

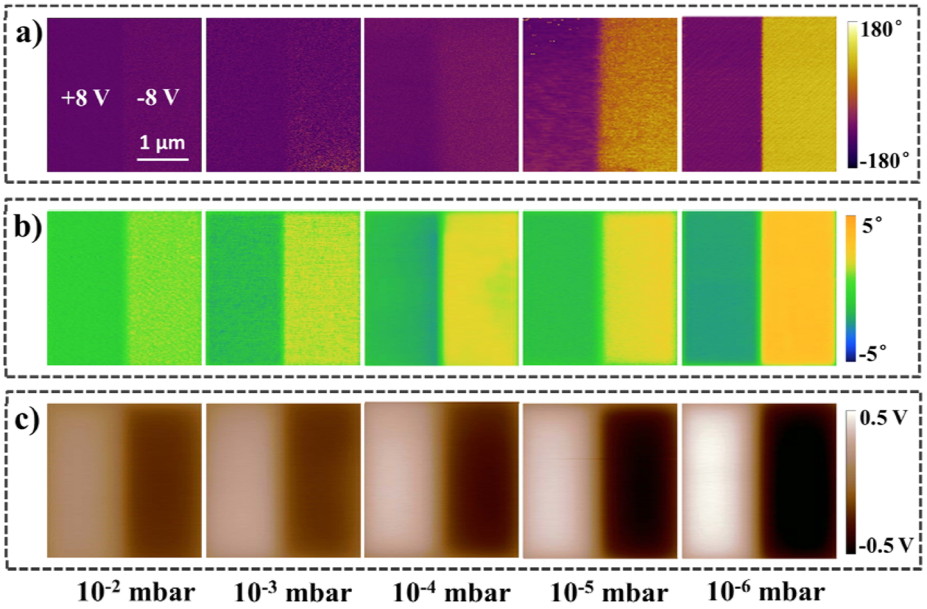

Figure 1. PFM (a), EFM (b), and SKPM (c) images of domains patterned on LAO/STO heterostructures deposited with an oxygen chamber pressure of 10^{-2}, 10^{-3}, 10^{-4}, 10^{-5}, or 10^{-6} mbar.

thick LAO/STO samples exhibit a metallic interface with a typical sheet resistance of 10^4 Ω/□ at room temperature. An Asylum Research Cypher-ES atomic force microscope (AFM), equipped with an environment cell, was used from surface morphology and electromechanical characterizations. A prescribed amount of water was introduced into the environmental cell and was heated to be fully evaporated. Vapor pressure and relative humidity at various temperatures were obtained via calculation. Pt/Ir conductive tips (EFM, Nanoworld) were employed. The nominal force constant of the cantilever is 2.8 N/m, and its resonant frequency in air is around 75 kHz. The in-contact resonant frequency on LAO/STO is in the range of 300−320 kHz. Before each measurement, the samples were heated at 200 °C for 30 min in dry flowing N_2 to eliminate the influence from surface adsorbates[29−31,34] and then transferred immediately into the environment cell. Domains were written onto the LAO surface in the lithography mode by scanning the tip biased at 8.0 and −8.0 V, respectively, over two adjacent rectangles of 1.5 μm × 3.0 μm in area. Then PFM, EFM, and SKPM images were acquired over the two domains. PFM signals were sensed by applying a 1.0 V alternating voltage on the tip. EFM images were obtained with a +2.0 V dc read voltage, and SKPM images were obtained at a lift height of 30 nm away from the sample surface.

III. RESULTS AND DISCUSSION

Figure 1a shows PFM phase images of the domains written with 8.0 and −8.0 V, respectively, onto LAO/STO heterostructures deposited with various oxygen pressures from 10^{-6} to 10^{-2} mbar. PFM phase contrast between the two domains increases with decreasing chamber oxygen pressure during deposition. A nearly 180° phase change, indicative of a complete "polar" switching, is observed in LAO/STO deposited at 10^{-6} mbar oxygen pressure, while very weak phase contrast is observed for samples deposited with the oxygen pressure greater than 10^{-4} mbar. Clear PFM phase and amplitude hysteresis loops of these LAO/STO heterostructures can also be observed.[39] Electromechanical responses have been previously reported in crystallized as well as amorphous LAO films.[32,35,36] Bark et al.[32] revealed, from first-principle calculations, that there are two energy minima for oxygen vacancies in the LAO layer deposited on STO substrates. One is on the LAO/STO interface, and the other is near the LAO surface. Charged oxygen vacancies may migrate between these two minima under an applied voltage to produce an effective electric field in LAO, leading to the observed switchable electromechanical response.[32,35] Considering that oxygen deficiency may be more severe in LAO films deposited with a lower oxygen chamber pressure, the observation in Figure 1a demonstrates that oxygen vacancies are indeed responsible for the observed electromechanical response and that the concentration of oxygen vacancies has an important effect.

Charges on LAO surface after domain patterning are checked by EFM and SKPM, as shown in Figure 1b and c, respectively. The phase contrast in EFM comes from the Coulomb interaction between the surface charges and the positively charged AFM tip. Dark contrast in Figure 1b, which indicates a retarded cantilever oscillation, corresponds to a positive surface charge. On the contrary, bright contrast corresponds to a negative surface charge.[32] This implies that a positive writing bias leaves positive charges on the surface, while a negative writing bias leaves negative ones. This is also supported by the SKPM results, where areas scanned with a positive (negative) bias exhibit a positive (negative) potential against the tip. The sign of surface charges after domain patterning is consistent with previous results,[32] where it is ascribed to screening from the ambient to compensate the effective poling in LAO due to oxygen vacancy migration.

Figure 2 shows the extracted EFM and SKPM contrast values as functions of oxygen pressure during LAO deposition. The contrast values are obtained by average over the positive and the negative domains. The increasing contrast with decreasing oxygen pressure in both EFM and SKPM images indicates that there are more charges on the LAO surface after domain patterning in samples deposited at lower oxygen pressure. This again supports the arguments that oxygen vacancy migration may produce an effective electric field in LAO and that the amplitude of the field increases with increasing oxygen vacancy concentration. The low oxygen vacancy concentration, in LAO/STO heterostructures deposited with an oxygen pressure greater than 10^{-4} mbar, is not enough to generate a significant electromechanical signal. It has been reported that there is a

DOI: 10.1021/am509113j
ACS Appl. Mater. Interfaces 2015, 7, 10146−10151

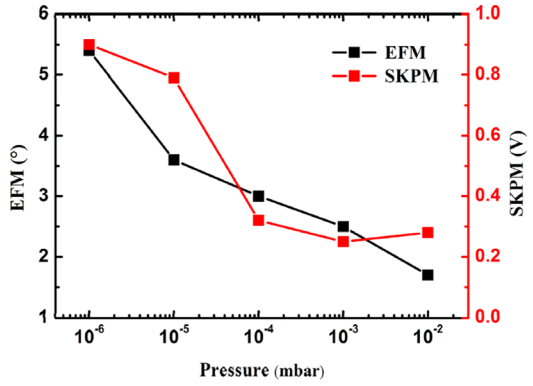

Figure 2. EFM and SKPM signals as functions of oxygen pressure during LAO deposition.

large electrostrictive coefficient, about 0.4 $Å^2/V^2$, in the LAO layer of LAO/STO heterostructures.[37] Bark et al.[32] attributed the observed electromechanical response to this intrinsic electrostriction, biased by a bistable electric field induced by the distribution of oxygen vacancies in LAO. These authors ruled out contributions from the surface charge by the observation of PFM signals from a Pt electrode deposited on the LAO/STO heterostructure. However, surface charges on bare LAO/STO heterostructures do produce an additional electric field and may modulate the electrostriction in the LAO layer. For example, Xie et al.[34] observed a ferroelectric-like hysteresis from LAO/STO and ascribed it to tip-induced electron injection or surface water ionization. Huang et al.[33] reported that ionic adsorbates on LAO/STO may enhance the electromechanical response, which is not observable in vacuum.

We then study the effects of surface charges on the electromechanical response of LAO/STO heterostructures by performing PFM measurements in various water vapor ambient at temperatures from 30 to 110 °C. The samples are deposited at 10^{-3} mbar oxygen pressure, which exhibit nearly no electromechanical response in air, as shown in Figure 2. Earlier reports indicate that water molecules bind to LAO surface strongly and dissociate into positively charged hydrogen ions and negatively charged hydroxyl ions. During domain patterning, the charged PFM tips remove one of them selectively and leave the other on the surface.[34,38]

As shown in Figure 3, PFM phase contrast appears when water vapor is introduced. It increases with increasing amount of water introduced at a certain temperature but decreases with increasing temperature with a certain amount of water sealed in the environmental cell. The density of water molecules on LAO surface is determined by the competition between adsorption and desorption. By increasing the water vapor pressure at a certain temperature (via introducing more water), adsorption is enhanced while desorption is depressed. When temperature is increased while maintaining the amount of water, desorption is enhanced because water molecules now have more thermal energy to escape the surface. Considering that high humidity may influence the resonant frequency between tip and sample, the PFM drive frequency we used is adjusted with the changes of the temperature and humidity.[39] The observations in Figure 3 indicate that surface charges adsorbed on LAO surface do have effects on the observed electromechanical response. More water molecules adsorbed, stronger PFM phase contrast observed.

This is shown in Figure 4, where the phase contrast increases linearly from 10 to 180° with the increase of relative humidity in the environmental cell, calculated from the measured pressure and the saturate pressure of water at a given temperature. It has also been observed that the electromechanical response from LAO/STO seems irrelevant to the interface two-dimensional conductibility. Domain patterning in water vapor on a 2 u.c.-thick LAO/STO sample with an insulating interface, deposited in 10^{-3} mbar oxygen, generates similar results.[39] Huang et al.[33] have reported the observed piezoelectric response is connected with the interfacial conductivity of LAO/STO samples. Note that samples in our experiments are not grounded and the interface and surface of the samples are not connected; the different observation

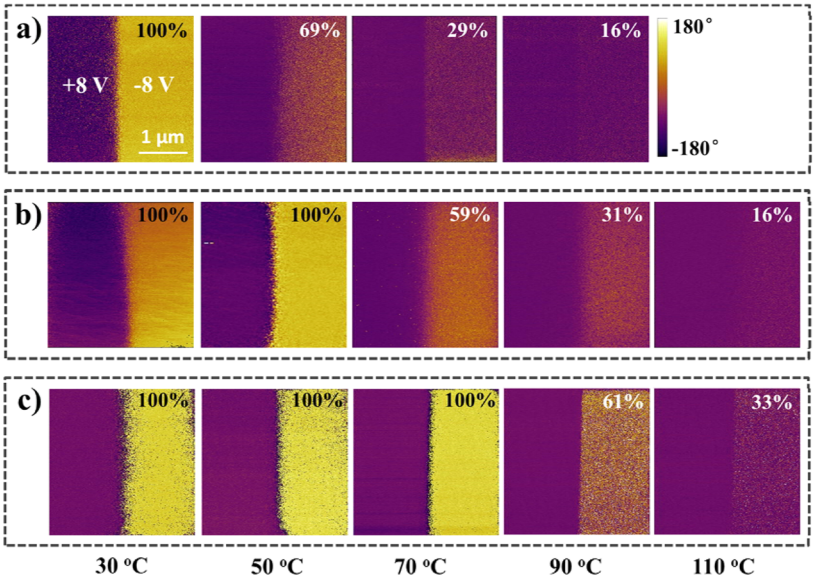

Figure 3. PFM images of domains patterned on LAO/STO heterostructures, measured in water vapor of different pressures at 30, 50, 70, 90, and 110 °C. The sample was deposited in 10^{-3} mbar oxygen chamber pressure. The water vapor pressures at 30 °C are 7.5 (a), 15.0 (b), and 30.0 (c) kPa, respectively. Relative humidity values are reported at the upper right corner of each image.

DOI: 10.1021/am509113j
ACS Appl. Mater. Interfaces 2015, 7, 10146−10151

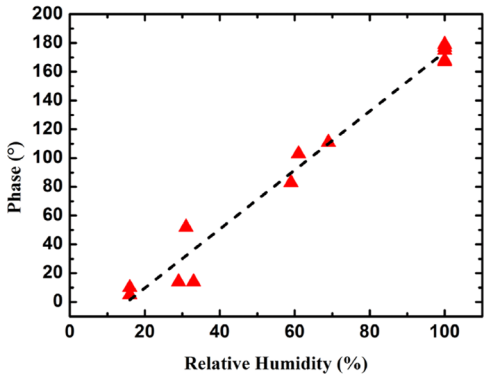

Figure 4. PFM phase contrast between domains patterned on LAO/STO heterostructures as a function of relative humidity. The sample was deposited in 10^{-3} mbar oxygen chamber pressure.

between us may be attributed to the different measurement methods.

Figure 5 shows PFM, EFM, and SKPM images of patterned domains on LAO/STO heterostructures deposited at 10^{-3} mbar, acquired in air and in water vapor. It is observed that charge density on LAO surface after domain patterning by ±8.0 V increases greatly by introducing water vapor. Excessive positive charges (probably H^+ ions) appear on areas scanned with a positively biased tip while excessive negative charges (probably OH^- ions) appear on areas scanned with a negatively biased tip.[38] In these LAO/STO samples deposited in high oxygen pressure, the effect of oxygen vacancies may be negligible. However, these surface charges produce an electric field that modulates the intrinsic electrostriction of LAO, which results in the observed PFM signal.

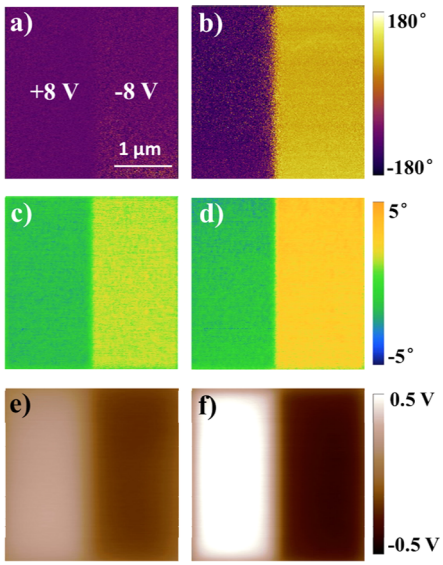

Figure 5. PFM (a, b), EFM (c, d), and SKPM (e, f) images of domains patterned on LAO/STO heterostructures deposited at 10^{-3} mbar, measured in air (a, c, e) and in water vapor (b, d, f).

The effect of patterning voltage is shown in Figure 6a and b. The domains are patterned by scanning a tip with a varying bias from 8.0 to −8.0 V with a −4.0 V interval, applied from the left to the right. The corresponding EFM and SKPM images acquired from the same area are shown in Figure 6c and d, respectively. It is clear that the sign of surface charges is

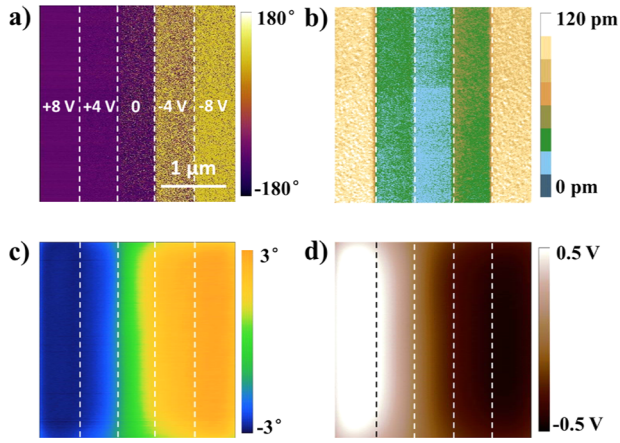

Figure 6. PFM phase (a), PFM amplitude (b), EFM (c), and SKPM (d) images of domains patterned on LAO/STO heterostructures deposited at 10^{-3} mbar, measured in water vapor. The domains are patterned by scanning a tip biased at 8.0, 4.0, 0, −4.0, and −8.0 V, from the left to the right.

determined by the polarity of the patterning voltage and surface charge density increases with increasing patterning voltage. PFM phase contrast between domains patterned by ±8.0 V is much stronger than that between domains patterned by ±4.0 V. PFM amplitude increases with increasing patterning voltage but independent of its polarity. This indicates that the observed PFM signal may come from the intrinsic electrostriction of LAO biased by an electric field induced by the surface charges. Surface charges induced during PFM writing process build an initial electric field E in LAO. During the PFM reading process, a sinusoidal drive signal is applied to the PFM tip. On the areas covered with positive charges, the positive voltage enhances the initial electric field while the negative voltage reduces the field; namely, the feedback signals have the same phase with the applied ones. On the areas covered with negative charges, the results are inverse. The polarity of the surface electric field results in the observed PFM phase contrast. The amplitude of the biased electrostriction is determined by the amplitude of the surface electric field, which in turn is determined by the surface charge density.

IV. CONCLUSIONS

In summary, electromechanical response from LAO/STO heterostructures, deposited with different oxygen chamber pressures, is studied as functions of temperature and ambient humidity. The observed electromechanical response is a result of intrinsic electrostriction in LAO, modulated by an additional electric field induced by oxygen vacancy redistribution or by adsorbed surface charges.[32,33] In samples with a high oxygen vacancy concentration (deposited in oxygen chamber pressure less than 10^{-5} mbar), migration of oxygen vacancies alone may produce a strong PFM signal. But in samples with less oxygen vacancies, the PFM signal increases with increasing concentration of surface ionic adsorbates, which increases with increasing ambient humidity.

■ ASSOCIATED CONTENT

Supporting Information

Details on RHEED oscillations, surface morphology, and the effect of LAO thickness. The Supporting Information is

DOI: 10.1021/am509113j
ACS Appl. Mater. Interfaces 2015, 7, 10146−10151

available free of charge on the ACS Publications website at DOI: 10.1021/am509113j.

AUTHOR INFORMATION

Corresponding Author

*E-mail: diwu@nju.edu.cn.

Notes

The authors declare no competing financial interest.

ACKNOWLEDGMENTS

This work was jointly sponsored by State Key Program for Basic Research of China (2015CB921203), Natural Science Foundation of China (51222206, 11374139 and U1432112), Jiangsu Provincial Natural Science Foundation (BK2012016), and Doctoral Foundation of Chinese Ministry of Education (20110091110013).

REFERENCES

(1) Ohtomo, A.; Hwang, H. Y. A High-Mobility Electron Gas at the $LaAlO_3/SrTiO_3$ Heterointerface. *Nature (London)* **2004**, *427*, 423 - 426.

(2) Nakagawa, N.; Hwang, H. Y.; Muller, D. A. Why Some Interfaces Cannot Be Sharp. *Nat. Mater.* **2006**, *5*, 204−209.

(3) Herranz, G.; Basletić, M.; Bibes, M.; Carrétéro, C.; Tafra, E.; Jacquet, E.; Bouzehouane, K.; Deralot, C.; Hamzić, A.; Broto, J.-M.; Barthélémy, A.; Fert, A. High Mobility in $LaAlO_3/SrTiO_3$ Heterostructures: Origin, Dimensionality, and Perspectives. *Phys. Rev. Lett.* **2007**, *98*, 216803.

(4) Siemons, W.; Koster, G.; Yamamoto, H.; Harrison, W. A.; Lucovsky, G.; Geballe, T. H.; Blank, D. H. A.; Beasley, M. R. Origin of Charge Density at $LaAlO_3$ on $SrTiO_3$ Heterointerfaces: Possibility of Intrinsic Doping. *Phys. Rev. Lett.* **2007**, *98*, 196802.

(5) Kalabukhov, A.; Gunnarsson, R.; Börjesson, J.; Olsson, E.; Claeson, T.; Winkler, D. Effect of Oxygen Vacancies in the $SrTiO_3$ Substrate on the Electrical Properties of the $LaAlO_3/SrTiO_3$ Interface. *Phys. Rev. B* **2007**, *75*, 121404 (R).

(6) Siemons, W.; Koster, G.; Yamamoto, H.; Geballe, T. H.; Blank, D. H. A.; Beasley, M. R. Experimental Investigation of Electronic Properties of Buried Heterointerfaces of $LaAlO_3$ on $SrTiO_3$. *Phys. Rev. B* **2007**, *76*, 155111.

(7) Chen, Y. Z.; Pryds, N.; Kleibeuker, J. E.; Koster, G.; Sun, J. R.; Stamate, E.; Shen, B. G.; Rijnders, G.; Linderoth, S. Metallic and Insulating Interfaces of Amorphous $SrTiO_3$-Based Oxide Heterostructures. *Nano Lett.* **2011**, *11*, 3774−3778.

(8) Santander-Syro, A. F.; Copie, O.; Kondo, T.; Fortuna, F.; Pailhés, S.; Weht, R.; Qiu, X. G.; Bertran, F.; Nicolaou, A.; Taleb-Ibrahimi, A.; Le Fèvre, P.; Herranz, G.; Bibes, M.; Reyren, N.; Apertet, Y.; Lecoeur, P.; Barthélémy, A.; Rozenberg, M. J. Two-Dimensional Electron Gas with Universal Subbands at the Surface of $SrTiO_3$. *Nature* **2011**, *469*, 189−193.

(9) Meevasana, W.; King, P. D. C.; He, R. H.; Mo, S. K.; Hashimoto, M.; Tamai, A.; Songsiriritthigul, P.; Baumberger, F.; Shen, Z. X. Creation and Control of a Two-Dimensional Electron Liquid at the Bare $SrTiO_3$ Surface. *Nat. Mater.* **2011**, *10*, 114−118.

(10) Sambri, A.; Cristensen, D. V.; Trier, F.; Chen, Y. Z.; Amoruso, S.; Pryds, N.; Bruzzese, R.; Wang, X. Plasma Plume Effects on the Conductivity of Amorphous-$LaAlO_3/SrTiO_3$ Interfaces Grown by Pulsed Laser Deposition in O_2 and Ar. *Appl. Phys. Lett.* **2012**, *100*, 231605.

(11) Liu, Z. Q.; Li, C. J.; Lü, W. M.; Huang, X. H.; Huang, Z.; Zeng, S. W.; Qiu, X. P.; Huang, L. S.; Annadi, A.; Chen, J. S.; Coey, J. M. D.; Venkatesan, T.; Ariando. Origin of the Two-Dimensional Electron Gas at $LaAlO_3/SrTiO_3$ Interfaces: The Role of Oxygen Vacancies and Electronic Reconstruction. *Phys. Rev. X* **2013**, *3*, 021010.

(12) Willmott, P. R.; Pauli, S. A.; Herger, R.; Schlepütz, C. M.; Martoccia, D.; Patterson, B. D.; Delley, B.; Clarke, R.; Kumah, D.; Cionca, C.; Yacoby, Y. Structural Basis for the Conducting Interface between $LaAlO_3$ and $SrTiO_3$. *Phys. Rev. Lett.* **2007**, *99*, 155502.

(13) Breckenfeld, E.; Bronn, N.; Karthik, J.; Damodaran, A. R.; Lee, S.; Mason, N.; Martin, L. W. Effect of Growth Induced (Non)-Stoichiometry on Interfacial Conductance in $LaAlO_3/SrTiO_3$. *Phys. Rev. Lett.* **2013**, *110*, 196804.

(14) Sato, H. K.; Bell, C.; Hikita, Y.; Hwang, H. Y. Stoichiometry Control of the Electronic Properties of the $LaAlO_3/SrTiO_3$ Heterointerface. *Appl. Phys. Lett.* **2013**, *102*, 251602.

(15) Reyren, N.; Thiel, S.; Caviglia, A. D.; Kourkoutis, L. F.; Hammerl, G.; Richter, C.; Schneider, C. W.; Kopp, T.; Rüetschi, A. S.; Jaccard, D.; Gabay, M.; Muller, D. A.; Triscone, J. M.; Mannhart, J. Superconducting Interfaces between Insulating Oxides. *Science* **2007**, *317*, 1196−1199.

(16) Reyren, N.; Gariglio, S.; Caviglia, A. D.; Jaccard, D.; Schneider, T.; Triscone, J.-M. Anisotropy of the Superconducting Transport Properties of the $LaAlO_3/SrTiO_3$ Interface. *Appl. Phys. Lett.* **2009**, *94*, 112506.

(17) Brinkman, A.; Huijben, M.; Van Zalk, M.; Huijben, J.; Zeitler, U.; Maan, J. C.; Van Der Wiel, W. G.; Rijnders, G.; Blank, D. H. A.; Hilgenkamp, H. Magnetic Effects at the Interface between Non-magnetic Oxides. *Nat. Mater.* **2007**, *6*, 493−496.

(18) Ariando; Wang, X.; Baskaran, G.; Liu, Z. Q.; Huijben, J.; Yi, J. B.; Annadi, A.; Roy Barman, A.; Rusydi, A.; Dhar, S.; Feng, Y. P.; Ding, J.; Hilgenkamp, H.; Venkatesan, T. Electronic Phase Separation at the $LaAlO_3/SrTiO_3$ Interface. *Nat. Commun.* **2011**, *2*, 188.

(19) Li, L.; Richter, C.; Mannhart, J.; Ashoori, R. C. Coexistence of Magnetic Order and Two-Dimensional Superconductivity at $LaAlO_3/SrTiO_3$ Interfaces. *Nat. Phys.* **2011**, *7*, 762−766.

(20) Dikin, D. A.; Mehta, M.; Bark, C. W.; Folkman, C. M.; Eomand, C. B.; Chandrasekhar, V. Coexistence of Superconductivity and Ferromagnetism in Two Dimensions. *Phys. Rev. Lett.* **2011**, *107*, 056802.

(21) Bert, J. A.; Kalisky, B.; Bell, C.; Kim, M.; Hikita, Y.; Hwang, H. Y.; Moler, K. A. Direct Imaging of the Coexistence of Ferromagnetism and Superconductivity at the $LaAlO_3/SrTiO_3$ Interface. *Nat. Phys.* **2011**, *7*, 767−771.

(22) Michaeli, K.; Potter, A. C.; Lee, P. A. Superconducting and Ferromagnetic Phases in $SrTiO_3/LaAlO_3$ Oxide Interface Structures: Possibility of Finite Momentum Pairing. *Phys. Rev. Lett.* **2012**, *108*, 117003.

(23) Lee, J.-S.; Xie, Y. W.; Sato, H. K.; Bell, C.; Hikita, Y.; Hwang, H. Y.; Kao, C.-C. Titanium d_{xy} Ferromagnetism at the $LaAlO_3/SrTiO_3$ Interface. *Nat. Mater.* **2013**, *12*, 703−706.

(24) Banerjee, S.; Erten, O.; Randeria, M. Ferromagnetic Exchange, Spin−Orbit Coupling, and Spiral Magnetism at the $LaAlO_3/SrTiO_3$ Interface. *Nat. Phys.* **2013**, *9*, 626−630.

(25) Narayanapillai, K.; Gopinadhan, K.; Qiu, X. P.; Annadi, A.; Ariando; Venkatesan, T.; Yang, H. Current-Driven Spin Orbit Field in $LaAlO_3/SrTiO_3$ Heterostructures. *Appl. Phys. Lett.* **2013**, *105*, 162405.

(26) Park, J. W.; Bogorin, D. F.; Cen, C.; Felker, D. A.; Zhang, Y.; Nelson, C. T.; Bark, C. W.; Folkman, C. M.; Pan, X. Q.; Rzchowski, M. S.; Levy, J.; Eom, C. B. Creation of A Two-Dimensional Electron Gas at an Oxide Interface on Silicon. *Nat. Commun.* **2013**, *1*, 94.

(27) Kim, S.-I.; Kim, D.-H.; Kim, Y.; Moon, S. Y.; Kang, M.-G.; Choi, J. K.; Jang, H. W.; Kim, S. K.; Choi, J.-W.; Yoon, S.-J.; Chang, H. J.; Kang, C.-Y.; Lee, S.; Hong, S.-H.; Ki, J.-S.; Baek, S.-H. Non-Volatile Control of 2DEG Conductivity at Oxide Interfaces. *Adv. Mater.* **2013**, *25*, 4612−4617.

(28) Cen, C.; Thiel, S.; Hammerl, G.; Schneider, C. W.; Andersen, K. E.; Hellberg, C. S.; Mannhart, J.; Levy, J. Nanoscale Control of an Interfacial Metal−Insulator Transition at Room Temperature. *Nat. Mater.* **2008**, *7*, 298−302.

(29) Xie, Y. W.; Bell, C.; Hikitaand, Y.; Hwang, H. Y. Tuning the Electron Gas at an Oxide Heterointerface via Free Surface Charges. *Adv. Mater.* **2011**, *23*, 1744−1747.

(30) Xie, Y. W.; Hikita, Y.; Bell, C.; Hwang, H. Y. Control of Electronic Conduction at an Oxide Heterointerface Using Surface Polar Adsorbates. *Nat. Commun.* **2011**, *2*, 494.

(31) Au, K.; Li, D. F.; Chan, N. Y.; Dai, J. Y. Polar Liquid Molecule Induced Transport Property Modulation at $LaAlO_3/SrTiO_3$ Heterointerface. *Adv. Mater.* **2012**, *24*, 2598−2602.
(32) Bark, C. W.; Sharma, P.; Wang, Y.; Baek, S. H.; Lee, S.; Ryu, S.; Folkman, C. M.; Paudel, T. R.; Kumar, A.; Kalinin, S. V.; Sokolov, A.; Tsymbal, E. Y.; Rzchowski, M. S.; Gruverman, A.; Eom, C. B. Switchable Induced Polarization in $LaAlO_3/SrTiO_3$ Heterostructures. *Nano Lett.* **2012**, *12*, 1765−1771.
(33) Huang, M.; Bi, F.; Bark, C. W.; Ryu, S.; Cho, K.-H.; Eom, C.-B.; Levy, J. Non-Local Piezoresponse of $LaAlO_3/SrTiO_3$ Heterostructures. *Appl. Phys. Lett.* **2014**, *104*, 161606.
(34) Xie, Y. W.; Bell, C.; Yajima, T.; Hikita, Y.; Hwang, H. Y. Charge Writing at the $LaAlO_3/SrTiO_3$ Surface. *Nano Lett.* **2010**, *10*, 2588−2591.
(35) Kumar, A.; Arruda, T. M.; Kim, Y.; Ivanov, I. N.; Jesse, S.; Bark, C. W.; Bristowe, N. C.; Artacho, E.; Littlewood, P. B.; Eom, C.-B.; Kalinin, S. V. Probing Surface and Bulk Electrochemical Processes on the $LaAlO_3$−$SrTiO_3$ Interface. *ACS Nano* **2012**, *6*, 3841−3852.
(36) Borowiak, A. S.; Baboux, N.; Albertini, D.; Vilquin, B.; Saint Girons, G.; Pelloquin, S.; Gautier, B. Electromechanical Response of Amorphous $LaAlO_3$ Thin Film Probed by Scanning Probe Microscopies. *Appl. Phys. Lett.* **2014**, *105*, 012906.
(37) Cancellieri, C.; Fontaine, D.; Gariglio, S.; Reyren, N.; Caviglia, A. D.; Fête, A.; Leake, S. J.; Pauli, S. A.; Willmott, P. R.; Stengel, M.; Ghosez, Ph.; Triscone, J.-M. Electrostriction at the $LaAlO_3/SrTiO_3$ Interface. *Phys. Rev. Lett.* **2011**, *107*, 056102.
(38) Bi, F.; Bogorin, D. F.; Cen, C.; Bark, C. W.; Park, J.-W.; Eom, C.-B.; Levy, J. Water-Cycle Mechanism for Writing and Erasing Nanostructures at the $LaAlO_3/SrTiO_3$ Interface. *Appl. Phys. Lett.* **2010**, *97*, 173110.
(39) See Supporting Information for details on RHEED oscillations, surface morphology, the effect of LAO thickness, PFM tip/sample approach curves under different humidity, drive frequency shift under different temperature and humidity, and phase and amplitude hysteresis loops of LAO/STO heterostructures deposited under different oxygen pressure.

DOI: 10.1021/am509113j
ACS Appl. Mater. Interfaces 2015, 7, 10146−10151